Sound-Evoked Radial Strain in the Hearing Organ

Igor Tomo, Jacques Boutet de Monvel, and Anders Fridberger
Karolinska Institutet, Center for Hearing and Communication Research, Departments of Clinical Neuroscience and Otolaryngology, M1, Karolinska University Hospital, SE-171 76 Stockholm, Sweden

ABSTRACT The hearing organ contains sensory hair cells, which convert sound-evoked vibration into action potentials in the auditory nerve. This process is greatly enhanced by molecular motors that reside within the outer hair cells, but the performance also depends on passive mechanical properties, such as the stiffness, mass, and friction of the structures within the organ of Corti. We used resampled confocal imaging to study the mechanical properties of the low-frequency regions of the cochlea. The data allowed us to estimate an important mechanical parameter, the radial strain, which was found to be 0.1% near the inner hair cells and 0.3% near the third row of outer hair cells during moderate-level sound stimulation. The strain was caused by differences in the motion trajectories of inner and outer hair cells. Motion perpendicular to the reticular lamina was greater at the outer hair cells, but inner hair cells showed greater radial vibration. These differences led to deformation of the reticular lamina, which connects the apex of the outer and inner hair cells. These results are important for understanding how the molecular motors of the outer hair cells can so profoundly affect auditory sensitivity.

INTRODUCTION

Sound causes vibration of the hearing organ. At low stimulus levels, these vibrations are the result of a complex interaction between the passive mechanical properties of the hearing organ, such as its stiffness, and the active force-generating capabilities of the outer hair cells. Fast force production by outer hair cells occurs through the membrane protein prestin (1–3) and through the transduction channel-based motors (4,5).

The mechanical parameters of the structures that surround the hair cells are functionally important. If surrounding structures were very stiff, forces produced by outer hair cells might be unable to enhance the sound-evoked vibrations. Similar problems might occur if the structures were too compliant. The stiffness has been measured for several structures within the organ of Corti (6–11). Although the mechanical properties of each cellular element are important, it is also essential to understand how these elements interact when subjected to the forces that develop during sound stimulation. Knowledge about cellular interactions during sound stimulation remains scant. Such interactions are difficult to probe with methods that measure the motion of a single point at a time. Multipoint measurements are based on either video microscopy (12,13) or rapid confocal imaging (14–16). During low-frequency stimulation with a stiff probe, the cochlear partition did appear to vibrate as a single rigid body (12). Rigid vibration was also seen in an excised turn of the gerbil cochlea (17). In contrast, during intense sound stimulation, the organ of Corti showed clear evidence of nonrigid motion (14). Electrical stimulation elicits nonrigid motion of the reticular lamina (18,19), but it is not clear whether this also occurs during sound stimulation at functionally relevant intensities. If that were the case, such slight deformations may trigger active mechanical responses from the hair cells (20,21).

This study was undertaken to investigate the mechanical properties of the cochlear partition. We used resampled confocal imaging to examine the motion of both inner and outer hair cells during moderate-level sound stimulation. The results are important for understanding the mechanisms underlying cochlear amplification and excitation of the inner hair cells.

METHODS

Animal preparation

The procedures used for preparing the temporal bones for these studies were described in previous reports (16,22,23). In brief, young guinea pigs were anesthetized and decapitated, and their temporal bones rapidly removed, using procedures approved by the local ethics committee (permit N311/03). The bulla was opened, and the preparation was attached to a holder with the external auditory meatus facing a loudspeaker. The preparation was immersed in tissue culture medium (minimum essential medium with Hank's salts, without L-glutamine, Gibco, Paisley, Scotland). A thin piece of plastic tubing was inserted in the scala tympani of the basal turn. The tubing was connected to a reservoir filled with oxygenated tissue culture medium, which flowed through scala tympani driven by gravity. A second opening at the cochlear apex served as the outlet for the medium and also permitted visualization of the organ of Corti. The sensory hair cells and auditory nerve dendrites were labeled with the styryl dye RH795. Supporting cells were visualized using the cytoplasmic dye calcein/AM (both dyes provided by Molecular Probes, Leiden, The Netherlands). Reissner's membrane was intact in all of the current experiments. Ionic concentrations in the scala media should therefore be very close to their normal values. This also means that the tectorial membrane and stereocilia are very weakly labeled, as the dyes do not have access to structures inside the scala media. This weak labeling precludes direct measurements of stereocilia deflection in most cases, but the current work is focused on measuring vibrations of other cellular elements. Previous work

Submitted February 2, 2007, and accepted for publication June 22, 2007.

Address reprint requests to Dr. Anders Fridberger, M1, Karolinska University Hospital Solna, SE 171 76 Stockholm, Sweden. Tel.: 46-8-51773274; Fax: 46-8-348546; E-mail: anders.fridberger@ki.se.

Editor: Herbert Levine.

0006-3495/07/11/3279/06 $2.00

doi: 10.1529/biophysj.107.105072

(16) showed that the tectorial membrane retains its normal position if the scala media is intact or, in cases of intentional rupture, if the medium outside the scala media is replaced with an endolymph-like solution.

The preparation was mounted on the stage of a laser scanning confocal microscope (LSM 510, Zeiss, Jena, Germany) and visualized with water immersion optics (Achroplan 40×, Zeiss, numerical aperture 0.8).

The isolation procedure interrupts blood flow to the preparation, resulting in a reduction of the endocochlear potential, which approaches zero some time after isolation. This decreases the driving force for ions entering hair cells and diminishes the effectiveness of the ''cochlear amplifier''. Vibrations described in this article are therefore dominated by passive mechanics. These passive mechanical properties are important for sound perception at all stimulus intensities (see Discussion). The reduced activity of the cochlear amplifier means that frequency tuning and response amplitudes may be lower than those found in vivo. However, the mechanical properties of the hearing organ are likely very close to those found in vivo, as the preparation sustains cochlear microphonic potentials (24) and the frequency tuning is similar to that found in in vivo recordings of receptor potentials (22; see also Fig. 1).

The immersion of the preparation in tissue culture medium and the opening of the apical turn of the cochlea reduce the effective sound pressure by ~20 dB (25). Sound pressures given below were not corrected for this attenuation.

Resampled imaging

The confocal microscope acquired images by scanning a laser beam across the focal plane of the objective lens. The frame rate is too low to directly visualize sound-evoked motions, which occurred at up to 500 Hz in the current study. However, pixels were acquired at a rate of ~250 kHz; each individual pixel is therefore unaffected by the motion artifacts that become quite apparent when a full frame is observed. For that reason, we designed custom data acquisition software tracking the temporal relation between each pixel and the sound stimulus. The result is two arrays: one containing the images and one containing samples of the waveform that drives the loudspeaker. Both arrays have equal dimensions. To reconstruct a resampled image sequence free from motion artifacts, a Fourier series approach was used (26). Consider a structure with constant fluorescence undergoing periodic motion in the plane of the image. Motion will make this object travel from one pixel into an adjacent one and back again, causing variations in pixel brightness over time. The motion may therefore be reconstructed by computing the Fourier series coefficients for each pixel along the time dimension. Two harmonics were found to be sufficient for accurate reconstructions. This means that the image sequence is low-pass filtered along the time dimension, resulting in substantially lower noise and better motion estimation than our previously used reconstruction technique (16). The previous technique was based on searching the arrays for pixels with similar phase values. In this study, the data acquisition system was further developed to support the acquisition of 512 × 512 pixel images at stimulus frequencies ranging from 100 to 500 Hz, the frequency range where the currently imaged cochlear region is maximally sensitive.

Calibration experiments were conducted using a small piece of fluorescent plastic attached to a feedback-controlled piezoelectric translator (P-841.10, Physik Instrumente, Karlsruhe, Germany). These experiments showed that motion amplitudes on the order of the pixel size and larger were measured with magnitude errors below 10% and angular errors of a few degrees (26). For motions smaller than the pixel size, the errors increase. The lower limit of practically useful measurements is ~20% of the pixel size (10–40 nm, depending on the zoom factor of the confocal microscope). The pixel size was adjusted according to the expected magnitude of the motion.

By tilting the preparation with respect to the optical axis of the microscope, we obtained images close to true cross sections. The exact angle was quantified by acquiring a series of images spaced by 1–3 μm along the z axis. This angle was usually ~20° with respect to the optical axis of the system. With such an orientation, the major axis of vibration is in the plane of the image, the above-mentioned angle causing an ~5% projection error. No correction was applied for this. In many experiments, the motions of inner and outer hair cells from the same focal plane were compared. In this case, both cell types were equally affected by the projection error.

Custom Matlab (the Mathworks, Natick, MA) programs were used for image processing. The image sequence was filtered with a three-dimensional Gaussian kernel. This operation was implemented in the frequency domain; it therefore assumed circular boundary conditions (i.e., that the motion of the hearing organ is strictly periodic). Deviations from periodicity would be lost in this processing step. Such deviations may occur as the result of noise or other factors, but they are expected to be small compared to the sound-evoked motions. The filtered image sequence was fed into a wavelet-based optical flow algorithm (15). This resulted in a motion estimate for each pixel within the image sequence.

To compare the directions of motion in different preparations, the angle of the reticular lamina with respect to the image x axis was measured. The data were then brought into a common coordinate system using affine transformation of the computed motion vectors.

Statistical analysis

Some of the data described below had non-Gaussian distribution. Therefore, nonparametric statistical tests were used throughout.

RESULTS

Frequency dependence

Tuning curves were acquired from the organ of Corti in 28 different preparations. One such curve, for stimulus frequencies between 100 and 300 Hz, is shown in Fig. 1 *B* (*asterisks*). An example image from this data set is shown in Fig. 1 *A*; the asterisk on the image indicates the location where the displacements shown in Fig. 1, *B–D* were measured. This particular image was acquired during sound stimulation at 175 Hz and 93 dB sound pressure level (SPL) (note that the immersion of the preparation in tissue culture medium and the opening of the apical turn reduce the effective SPL, as mentioned above). Although passive mechanics may dominate the response of the preparation, the frequency tuning is nonetheless comparable to that found in the receptor potentials of apical turn inner hair cells in vivo (*squares* in Fig. 1 *B*; data redrawn from Dallos (27)). For the region around the peak, the slopes of the two curves appear quite similar. The peak response was at 150 Hz; best frequencies ranged between 150 and 225 Hz in the current dataset.

Trajectories such as the ones shown in Fig. 1, *C* and *D*, may be analyzed by their eccentricity, defined as:

$$eccentricity = \sqrt{1 - \frac{(length\ of\ minor\ axis)^2}{(length\ of\ major\ axis)^2}}.$$

This dimensionless number would be 0 for a circle and 1 for a straight line, and it provides a means of quantifying trajectory shapes. At 175 Hz, trajectories were almost perfect lines, where the cell moved along a single, well-defined path (Fig. 1 *C*). At 275 Hz, motion directed at the scala vestibuli (*top of the image*) occurred along a different path from that seen during motion toward the scala tympani. The trajectory

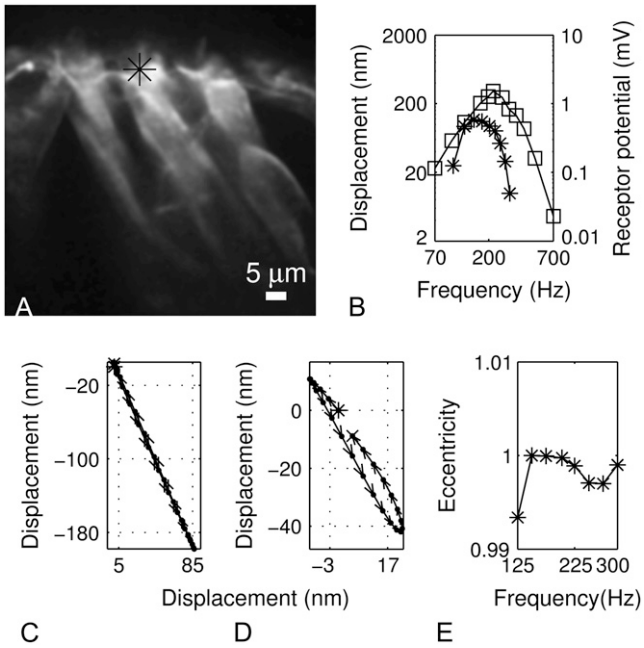

FIGURE 1 Tuning curves and motion trajectories from a second-row outer hair cell in situ. (*A*) Confocal image obtained during simultaneous sound stimulation. (*B*) A mechanical tuning curve (*, *scale on the left*) is plotted together with a fourth-turn inner hair cell receptor potential tuning curve redrawn from previously published data (□, *scale on the right*) (27). Peak displacement, 114 nm. (*C*) Trajectory at 150 Hz. Eccentricity, 1. (*D*) Trajectory at 275 Hz. Eccentricity, 0.997. The length of the major axis was obtained by computing the distance between the two extremes on the trajectories. The minor axis length is then obtained by measuring the length of a line drawn through the center of the trajectory, perpendicular to the first line. In all figures in this article, the origin of the trajectories is marked with an asterisk, which corresponds to phase zero of the voltage that drives the loudspeaker. (*E*) Trajectory eccentricities at different stimulus frequencies.

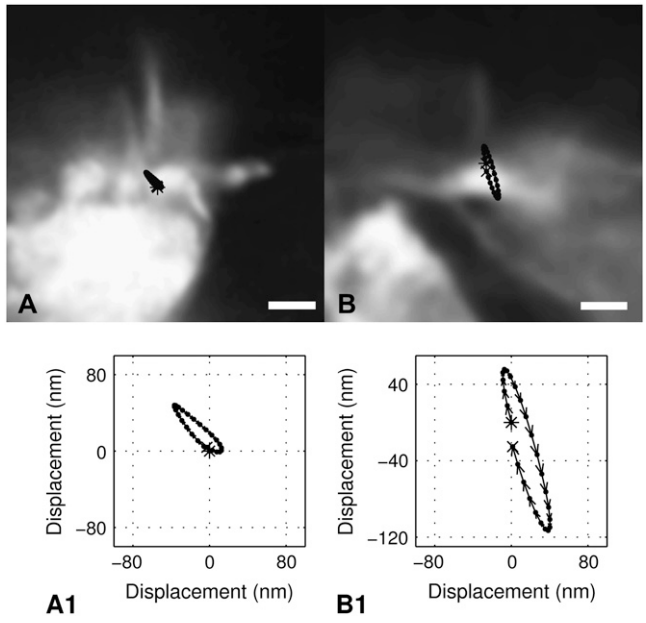

FIGURE 2 Vibrations of an inner and an outer hair cell from the same location within the cochlea. (*A*) An inner hair cell with a motion trajectory superimposed on the image. The trajectory is also shown in panel *A1*. (*B*) A third-row outer hair cell. Scale bars equal 3 μm for the images and 150 nm for the trajectories. Stimulus level, 93 dB SPL.

therefore begins to resemble an oval (Fig. 1 *D*). Fig. 1 *E* shows that eccentricity was high in the region around the best frequency and lower on either side of the peak. Across the entire data set, significant differences were found between trajectory eccentricities measured at 125, 150, and 175 Hz and those measured above 250 Hz (Kruskal-Wallis test, $p < 0.01$, $\chi^2 = 80.22$). There was also a tendency for inner hair cells to have lower eccentricity.

Thus, both the vibration amplitude and the trajectory shape depended on the stimulus frequency, but this was not the case for the main axis of vibration. Trajectory orientations were the same regardless of stimulus frequency ($p = 0.85$; Kruskal-Wallis test). However, the direction of vibration was dependent on the cell type.

Trajectory orientations differ in outer and inner hair cells

The main trajectory axis was different at the inner and outer hair cells. An example is shown in Fig. 2. The image of the inner hair cell in Fig. 2 *A* was acquired during sound stimulation at 203 Hz. The trajectory superimposed on the image is magnified 20× relative to the pixel size of the image; this trajectory is also displayed below the image in panel *A1*. The peak-to-peak displacement of this cell was 70 nm. Note that the main axis of the trajectory was inclined with respect to the reticular lamina. If the direction of the image *x* axis is defined as 0° and the image *y* axis as +90°, the trajectory angle was 134°.

The cells shown in Fig. 2 *B* came from the same location within the cochlea as the cell in Fig. 2 *A*, and identical stimulus parameters were used during image acquisition, but the trajectory from the third row outer hair cell was distinctly different from its inner hair cell counterpart. The main axis of the trajectory had an inclination of 105°, and the peak-to-peak amplitude was 180 nm. These are vibration amplitudes similar to those found in living anesthetized guinea pigs at ~70–75 dB SPL (28). When all inner and outer hair cells, regardless of stimulus frequency and level, were compared, the median difference in trajectory orientation was 12°. This difference was significant, as assessed with the Wilcoxon rank sum test ($p = 0.0001$ for the comparison between 129 inner hair cells and 243 third-row outer hair cells). The difference in trajectory orientation therefore appears as a robust phenomenon that occurs across the range of frequencies and intensities used here. Trajectory orientations changed gradually across the reticular lamina. Thus, first- and second-row outer hair cells had trajectory orientations intermediate between those of inner hair cells and third- row outer hair cells.

The reticular lamina is a continuous structure linking the apex of the sensory hair cells in a plate-like formation generally believed to be quite stiff. These data show that adjacent parts of this structure vibrate in dissimilar directions. Such a difference suggests that motion may be accompanied by deformation.

Compression and strain in the reticular lamina

To assess a possible deformation, all trajectories were first brought into a common coordinate system where the reticular lamina was oriented along the horizontal axis of the image. Vibration along this axis was determined by projection of the trajectories. In the ensuing text, this direction is termed ''radial''; the vibration component directed perpendicular to the reticular lamina is the transverse one (Fig. 3 *A*). Fig. 3 *B* shows the transverse vibration component in the inner and outer hair cell indicated on the image. In accordance with most other preparations in this series, the transverse vibration component had substantially higher amplitude in the outer hair cell (*dotted line*). Although a slight phase difference is seen between these waveforms, no such difference was found across all of the trajectories (median phase difference 0.3°).

Fig. 3 *C* shows the radial motion. Here, it is seen that the peak-to-peak radial displacement was 80 nm for the inner hair cell but only 30 nm for the outer hair cell. Thus, during motion toward the scala tympani, the inner hair cell moved further in the direction of the vascular stria than did the third-row outer hair cell. The distance between inner and outer hair cells therefore decreased, and the reticular lamina was compressed (Fig. 3 *D*). The relative amplitudes of these vibration components showed significant variability across frequencies and intensities. Nonetheless, when all the data were examined, the radial vibration component was on average 1.12 times larger in inner hair cells than in the third row of outer hair cells ($p = 0.035$ for the comparison between 91 cell pairs using the sign test). These data show that there is deformation of the reticular lamina during moderate-level sound stimulation because movements of the opposing ends of the same structure differ in size (there was no significant difference in the phase of the radial component measured at the outer and inner hair cells). The deformation showed no apparent dependence on stimulus frequency over the range used here (100–500 Hz).

A useful measure of deformation is the strain, obtained by dividing the length change by the initial distance between the two points. For the part of the reticular lamina between the inner hair cell and the first row of outer hair cells, the average strain was 0.1%. The segment between outer hair cells 1 and 2 showed an average strain of 0.2%, and that between outer hair cells 2 and 3 of 0.3%. The strain values for the segment between the inner hair cell and the first row of outer hair cells was significantly different from that between outer hair cell rows 1 and 2 ($p < 0.00001$ using the sign test). Because of a projection effect, an apparent compression or elongation of the reticular lamina could be observed in the image without actual deformation of this structure. However, calculations show that even for an angle of 40° between the radial and the image planes, the resulting strain (fictitious and of purely geometric origin) would be constant along the reticular lamina and much smaller (<0.02%) than the strains measured here. Thus, these data show that there is deformation of the reticular lamina and that most of it occurs near the outer hair cells.

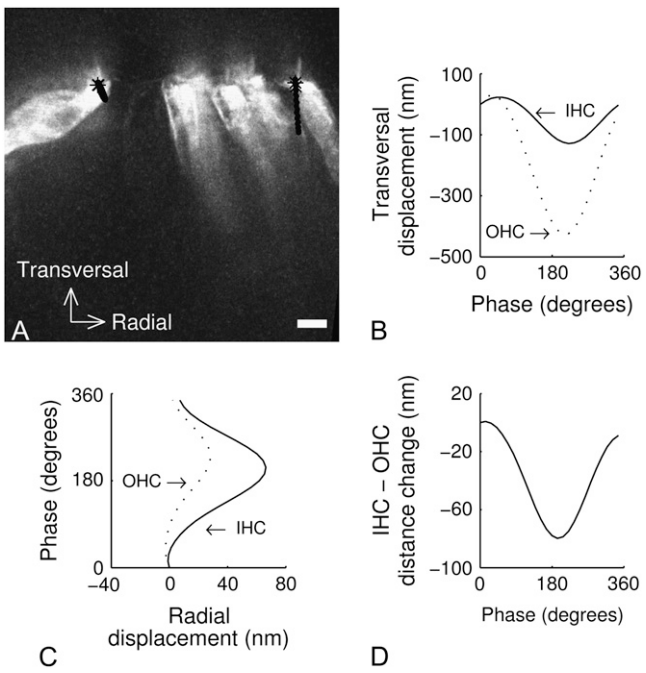

FIGURE 3 Transverse and radial vibration components in outer and inner hair cells. (*A*) Image obtained during sound stimulation at 200 Hz and 96 dB SPL. The scale bar equals 10 μm for the image and 250 nm for the trajectories. The transverse vibration component is shown in *B*, and the radial component in *C*. (*D*) The change in distance between the inner hair cell (IHC) and the third-row outer hair cell (OHC). The starting distance between the two cells was 65 μm.

DISCUSSION

In this study, we demonstrate that the passive mechanics of the hearing organ involve fast structural changes that lead to deformation of structures that are often considered to be relatively stiff. During moderate-level sound stimulation, the length of the reticular lamina changes. We also show that the structural alterations appear most pronounced near the outer hair cells because the mechanical strain is larger here. What relevance do these data have for our understanding of cochlear function?

Outer hair cells are known to change length after minute deformation of the cell membrane (20,29–31). This mechanical response depends on chloride ions; recent data show that such motility may contribute to amplifying the sound-evoked response of the hearing organ (21). A problem with

this theory is that deformations of the hearing organ were previously shown to occur only at very high stimulus levels or when electrical stimulation was used (14,18,32). Therefore, these results are important in showing that deformations do occur even for stimulation at moderate levels and for structures usually regarded as quite stiff.

Other theories have been proposed to explain the high sensitivity and frequency selectivity of the cochlea. A widely held theory involves outer hair cell electromotility, i.e., the control by the voltage-sensitive motor protein prestin (1) of outer hair cell length (2) and stiffness (33). Prestin may be driven either by the cell's receptor potential or by extracellular potential changes in the fluid spaces within the cochlea (34,35). Outer hair cell motility is assumed to augment organ of Corti vibrations. Obviously, such an amplifier is strongly dependent on the stiffness of structures surrounding the hair cells.

The transduction channel of the outer hair cell is also capable of rapid force generation (4), which may affect the vibration amplitude of the organ of Corti (5; however, see also Jia and He (36)). This motor sits between the reticular lamina and the tectorial membrane. The mechanical properties of both the reticular lamina and tectorial membrane would influence the performance of this mechanism.

Some mechanical parameters of the hearing organ are known. For instance, the average bending stiffness of pillar cells is 0.7 mN/m (37). If this value applies to the entire reticular lamina, an axial force of 56 pN is required to produce the 80-nm length change seen in Fig. 3. Pillar cells form a large part of the reticular lamina, but it should be noted that their stiffness in the radial direction might differ from the above value. Therefore, 56 pN is probably a lower bound on the force required to produce the reticular lamina deformations described here. A more realistic estimate may be achieved by considering the stress corresponding to the measured strain. Cai et al. (38) estimated Young's modulus of the reticular lamina to be 30 kPa. Assuming a homogeneous radial deformation, the radial stress would then be in the range 30–90 Pa. Because the diameter of an outer hair cell is $\sim$10 μm and the thickness of the cuticular plate is 1 μm, this would correspond to a radial force of 300–900 pN acting between two adjacent outer hair cells. These numbers can be compared to the force produced by hair cell motors. When stimulated electrically, individual outer hair cells generate a maximal force of 50–100 pN/mV (3,39). Measurements are also available for the hair bundle motor, which supplies a maximal force of $\sim$500 pN in rats (4). These numbers do suggest that reticular lamina deformation could occur in a cochlea driven by outer hair cell motility.

These deformations also mean that the organ of Corti is not vibrating in the classical near-rigid fashion seen in previous experiments (12,17). The study by Chan and Hudspeth showed large differences in radial motion between outer and inner hair cells. Radial motion was substantially larger at the inner hair cell and actually exceeded the transverse motion. Although we also find larger radial motion for the inner hair cell, it was never larger than the transverse vibration component. These differences may relate to differences in the mode of stimulation, as the Chan and Hudspeth preparation does not sustain normal traveling wave motion (5). It could also reflect the fact that our measurements were conducted in the cochlear apex, whereas Chan and Hudspeth did their measurements closer to the base.

The strain that we measured here (0.1–0.3%) is relatively small, but some cells can detect strains even smaller than these and respond by releasing prostaglandins and growth factors (40). Whether cells in the organ of Corti possess a similar capacity is not known.

Cellular mechanical properties have fundamental importance for the operation of the hearing organ. Previous attempts at modeling the behavior of this complex sensory system have had to infer such parameters from quasistatic data or data obtained during electrical stimulation. Nonetheless, these models provide very important insights and may also explain features of the current results. Thus, the increased strain demonstrated near outer hair cells could be a consequence of the curvature of the cochlea, which tends to concentrate energy near outer hair cells (41).

The purpose of all mechanical processes in the organ of Corti is to trigger transmitter release from inner hair cells onto auditory nerve dendrites. However, inner hair cell stereocilia lack firm contact with surrounding structures (42). Phase relations between the sound stimulus and the inner hair cell receptor potential suggested that inner hair cell stereocilia deflect because they interact with the surrounding fluid (43,44). This general concept was validated by recent direct measurements (16), but the exact nature of the fluid-structure interaction remains controversial. Active pumping of fluid toward hair bundles may occur (45), but deflection may also take place as the hair bundle is dragged through an otherwise inert fluid. Although the current study cannot resolve this issue, the larger radial vibration component measured at the inner hair cell may be important because it may contribute to deflection of inner hair cell stereocilia. In a sense, the passive mechanics appear to be optimized for stimulating inner hair cells.

Supported by stiftelsen Tysta Skolan, Hörselskadades Riksförbund, Åke Wibergs stiftelse, Karolinska Institutet, the Human Frontier Science Program, and the Swedish Research Council.

REFERENCES

1. Zheng, J., W. Shen, D. Z. He, K. B. Long, L. D. Madison, and P. Dallos. 2000. Prestin is the motor protein of cochlear outer hair cells. *Nature*. 405:149–155.
2. Brownell, W. E., C. R. Bader, D. Bertrand, and Y. de Ribaupierre. 1985. Evoked mechanical responses of isolated cochlear outer hair cells. *Science*. 227:194–196.
3. Frank, G., W. Hemmert, and A. W. Gummer. 1999. Limiting dynamics of high-frequency electromechanical transduction of outer hair cells. *Proc. Natl. Acad. Sci. USA*. 96:4420–4425.

4. Kennedy, H. J., A. C. Crawford, and R. Fettiplace. 2005. Force generation by mammalian hair bundles supports a role in cochlear amplification. *Nature*. 433:880–883.
5. Chan, D. K., and A. J. Hudspeth. 2005. Ca^{2+} current-driven nonlinear amplification by the mammalian cochlea in vitro. *Nat. Neurosci.* 8:149–155.
6. Zwislocki, J. J., and L. K. Cefaratti. 1989. Tectorial membrane II: stiffness measurements in vivo. *Hear. Res.* 42:211–228.
7. Scherer, M. P., and A. W. Gummer. 2004. Impedance analysis of the organ of Corti with magnetically actuated probes. *Biophys. J.* 87:1378–1391.
8. Olson, E. S., and D. C. Mountain. 1994. Mapping the cochlear partition's stiffness to its cellular architecture. *J. Acoust. Soc. Am.* 95:395–400.
9. Russell, I. J., and C. Schauz. 1995. Salicylate ototoxicity: effects on the stiffness and electromotility of outer hair cells isolated from the guinea pig cochlea. *Audit. Neurosci.* 1:309–320.
10. Tolomeo, J. A., C. R. Steele, and M. C. Holley. 1996. Mechanical properties of the lateral cortex of mammalian auditory outer hair cells. *Biophys. J.* 71:421–429.
11. Ulfendahl, M., E. Chan, W. B. McConnaughey, S. Prost-Domasky, and E. L. Elson. 1998. Axial and transverse stiffness measures of cochlear outer hair cells suggest a common mechanical basis. *Pflugers Arch.* 436:9–15.
12. Hu, X., B. N. Evans, and P. Dallos. 1999. Direct visualization of organ of Corti kinematics in a hemicochlea. *J. Neurophysiol.* 82:2798–2807.
13. Aranyosi, A. J., and D. M. Freeman. 2004. Sound-induced motions of individual cochlear hair bundles. *Biophys. J.* 87:3536–3546.
14. Fridberger, A., and J. Boutet de Monvel. 2003. Sound-induced differential motion within the hearing organ. *Nat. Neurosci.* 6:446–448.
15. Fridberger, A., J. Widengren, and J. Boutet de Monvel. 2004. Measuring hearing organ vibration patterns with confocal microscopy and optical flow. *Biophys. J.* 86:535–543.
16. Fridberger, A., I. Tomo, M. Ulfendahl, and J. Boutet de Monvel. 2006. Imaging hair cell transduction at the speed of sound: dynamic behavior of mammalian stereocilia. *Proc. Natl. Acad. Sci. USA.* 103:1918–1923.
17. Chan, D. K., and A. J. Hudspeth. 2005. Mechanical responses of the organ of Corti to acoustic and electrical stimulation in vitro. *Biophys. J.* 89:4382–4395.
18. Mammano, F., and J. F. Ashmore. 1993. Reverse transduction measured in the isolated cochlea by laser Michelson interferometry. *Nature*. 365:838–841.
19. Scherer, M. P., and A. W. Gummer. 2004. Vibration pattern of the organ of Corti up to 50 kHz: evidence for resonant electromechanical force. *Proc. Natl. Acad. Sci. USA.* 101:17652–17657.
20. Brundin, L., Å. Flock, and B. Canlon. 1989. Sound-induced motility of isolated cochlear outer hair cells is frequency-specific. *Nature.* 342: 814–816.
21. Santos-Sacchi, J., L. Song, J. Zheng, and A. L. Nuttall. 2006. Control of mammalian cochlear amplification by chloride anions. *J. Neurosci.* 26:3992–3998.
22. Ulfendahl, M., S. M. Khanna, A. Fridberger, Å. Flock, B. Flock, and W. Jäger. 1996. Mechanical response characteristics of the hearing organ in the low-frequency regions of the cochlea. *J. Neurophysiol.* 76:3850–3862.
23. Fridberger, A., Å. Flock, M. Ulfendahl, and B. Flock. 1998. Acoustic overstimulation increases outer hair cell Ca^{2+} concentrations and causes dynamic contractions of the hearing organ. *Proc. Natl. Acad. Sci. USA.* 95:7127–7132.
24. Fridberger, A., J. T. van Maarseveen, E. Scarfone, M. Ulfendahl, B. Flock, and Å. Flock. 1997. Pressure-induced basilar membrane position shifts and the stimulus-evoked potentials in the low-frequency region of the guinea pig cochlea. *Acta Physiol. Scand.* 161:239–252.
25. Franke, R., A. Dancer, S. M. Khanna, and M. Ulfendahl. 1992. Intracochlear and extracochlear sound pressure measurements in the temporal bone preparation of the guinea-pig. *Acustica.* 76:173–182.
26. Jacob, S., I. Tomo, A. Fridberger, J. Boutet de Monvel, and M. Ulfendahl. 2007. Rapid confocal imaging for measuring sound induced motion of the hearing organ in the apical region. *J. Biomed. Opt.* 12: 021005.
27. Dallos, P. 1986. Neurobiology of cochlear inner and outer hair cells: intracellular recordings. *Hear. Res.* 22:185–198.
28. Zinn, C., H. Maier, H. Zenner, and A. W. Gummer. 2000. Evidence for active, nonlinear, negative feedback in the vibration response of the apical region of the in-vivo guinea-pig cochlea. *Hear. Res.* 142: 159–183.
29. Brundin, L., and I. J. Russell. 1994. Tuned phasic and tonic motile responses of isolated outer hair cells to direct mechanical stimulation of the cell body. *Hear. Res.* 73:35–45.
30. Chan, E., and M. Ulfendahl. 1999. Mechanically evoked shortening of outer hair cells isolated from the guinea pig organ of Corti. *Hear. Res.* 128:166–174.
31. Rybalchenko, V., and J. Santos-Sacchi. 2003. Cl^- flux through a non-selective, stretch-sensitive conductance influences the outer hair cell motor of the guinea-pig. *J. Physiol.* 547:873–891.
32. Fridberger, A., J. Boutet de Monvel, and M. Ulfendahl. 2002. Internal shearing within the hearing organ evoked by basilar membrane motion. *J. Neurosci.* 22:9850–9857.
33. He, D. Z., and P. Dallos. 1999. Somatic stiffness of cochlear outer hair cells is voltage-dependent. *Proc. Natl. Acad. Sci. USA.* 96:8223–8228.
34. Dallos, P., and B. N. Evans. 1995. High-frequency motility of outer hair cells and the cochlear amplifier. *Science.* 267:2006–2009.
35. Fridberger, A., J. Boutet de Monvel, J. Zheng, N. Hu, Y. Zou, T. Ren, and A. L. Nuttall. 2004. Organ of Corti potentials and the motion of the basilar membrane. *J. Neurosci.* 24:10057–10063.
36. Jia, S., and D. Z. He. 2005. Motility-associated hair-bundle motion in mammalian outer hair cells. *Nat. Neurosci.* 8:1028–1034.
37. Tolomeo, J. A., and M. C. Holley. 1997. Mechanics of microtubule bundles in pillar cells from the inner ear. *Biophys. J.* 73:2241–2247.
38. Cai, H., B. Shoelson, and R. S. Chadwick. 2004. Evidence of tectorial membrane radial motion in a propagating mode of a complex cochlear model. *Proc. Natl. Acad. Sci. USA.* 101:6243–6248.
39. Iwasa, K. H., and M. Adachi. 1997. Force generation in the outer hair cell of the cochlea. *Biophys. J.* 73:546–555.
40. Ehrlich, P. J., and L. E. Lanyon. 2002. Mechanical strain and bone cell function: a review. *Osteoporos. Int.* 13:688–700.
41. Manoussaki, D., E. K. Dimitriadis, and R. S. Chadwick. 2006. Cochlea's graded curvature effect on low frequency waves. *Phys. Rev. Lett.* 96:088701.
42. Lim, D. J. 1986. Functional structure of the organ of Corti: a review. *Hear. Res.* 22:117–146.
43. Dallos, P., M. C. Billone, J. D. Durrant, C.-Y. Wang, and S. Raynor. 1972. Cochlear inner and outer hair cells: functional differences. *Science.* 177:356–358.
44. Russell, I. J., and P. M. Sellick. 1983. Low-frequency characteristics of intracellularly recorded receptor potentials in guinea-pig cochlear hair cells. *J. Physiol.* 338:179–206.
45. Nowotny, M., and A. W. Gummer. 2006. Nanomechanics of the subtectorial space caused by electromechanics of cochlear outer hair cells. *Proc. Natl. Acad. Sci. USA.* 103:2120–2125.